Steel and Composite Structures, Vol. 9, No. 1 (2009) 1-17
DOI: http://dx.doi.org/10.12989/scs.2009.9.1.001

Analysis of corrugated board panels under compression load

M.E. Biancolini*, C. Brutti and S. Porziani

Dipartimento di Ingegneria Meccanica, Università di Roma "Tor Vergata", Via del Politecnico 1, 00133 Roma, Italy

(Received September 28, 2006, Accepted May 8, 2008)

Abstract. This paper is focused on the buckling and post buckling behaviour of rectangular corrugated board panels simply supported and subjected to compression load. The aim of the work is to understand the failure mechanism of investigated structure in order to quantify the effect of design parameters on the strength of a panel of given geometry. Two numerical models were developed adopting the finite element method. In the first one the corrugated board is represented by means of shell elements adopting an equivalent material, in the second the local structure is described in full detail modelling both straight and corrugated layers by means of shell elements and representing the connection between layers by special interface elements. The model correctness was checked by the comparison between out of plane central displacement predicted by the models and the experimental values found in literature. For the same case the effect of panel planarity error was evaluated. Finally a parametric analysis to investigate the effect of design parameters was carried out.

Keywords : corrugated board; finite element analysis (FEA); micro-mechanics; buckling.

1. Introduction

Corrugated board is today the preferred choice in packaging sector because it is versatile and easily manufactured and it is also economic and ecological. A consistent part of produced goods in a country is shipped in corrugated board containers and so its consumption is a good index of national welfare (50.6 kg *pro capite* in Italy, 38.4 kg *pro capite* in Europe, year 2003, according to annual statistic of FEFCO).

Containers of various shapes are obtained starting from flat rectangular panels built with three or more paperboard layers. Assembled material performances are given by many factors as composition of each layer, corrugation shape, panel thickness, adhesive joints shape.

When the weight of packaged items is high the main strength requirement is the compression load due to containers stacking, usually denoted as BCT load (load obtained in Box Compression Testing according to FEFCO Test method 50, EN12048 or TAPPI T804).

A container is designed starting from the topologic problem because its internal room has to accommodate the products shape; beside that also the container external shape has to be properly defined in order to fit a standard pallet dimensions with an integer number of containers. Once box dimensions are defined the corrugated board composition has to be selected among the available ones looking for the minimum cost guarantying the ability to withstand the strength requirement.

BCT of the container depends on container global shape and on corrugated board strength and

* Corresponding Author, Email: biancolini@ing.uniroma2.it

stiffness. The simpler method for boxes design consists in the use of the simplified McKee design formula (Mckee *et al*. 1963).

$$BCT = 1.82ECT\sqrt{h}\sqrt{p} \tag{1}$$

Where *ECT* (the strength of a rectangular corrugated board specimen in Edge Compression Test and according to TAPPI T811 or ISO 3037 standards) can be measured or estimated from RCT of building papers (strength of a ring strip of paper specimen in Ring Compression Test measured according to ISO 12192) accordingly to the following equation:

$$ECT = RCT_{fluting}\ \psi + RCT_{liner1} + RCT_{liner2} \tag{2}$$

This approach is a very simple way to calculate BCT as a function of container shape and composition. Unfortunately this design formula works only once many parameters are tuned.

To gather the actual behaviour of a container under compression, a deep physical insight is required. A good starting point is to reconsider the original McKee contribution (Mckee *et al*. 1963) in which the BCT evaluation was performed by a theoretical analysis of eigenvalues buckling load of a box that is used to estimate the maximum post buckling load. According to McKee approach, overall container strength is obtained summing the contribution of lateral walls that can be easily modelled as simple rectangular panels. Following the same criterion a theoretical solution for the post-buckling behaviour of a corrugated board panel was recently presented by Nordstrand (2004).

In the last decades several contributions about corrugated board strength using a numerical approach based on FEM analysis were presented. A non linear FEM simulation, based on equivalent shell element, for the study of a box in post buckling behaviour was presented by Beldie *et al.* (2001). A further contribution for the collapse analysis of a complete container was given by Gilchrist *et al.* (1999) that presented a non linear FEM simulation at microscale level, i.e. representing the actual geometry of fluting and liners for the whole package.

Studies about corrugated board stiffness were presented by Pommier and Poustis (1990) with a contributions addressed to three point FEM simulation and Nordstrand and Carlsson (1997) with a comprehensive experimental and numerical investigation about bending and out of plane shear stiffness of corrugated board. Recently Aboura *et al.* (2004) presented a study in which measured stiffness properties of corrugated board panels were reproduced by an equivalent element obtained with a theoretical solution and verified by micromechanical FEM simulations.

A study about lateral crushing, conducted both experimentally and numerically, was presented by Lu *et al*. (2001) proposing a shape optimisation for the fluting to improve the strength against the crushing that occurs during product processing.

A numerical approach, based on FEM analysis of a box to estimate buckling load, after the evaluation of equivalent moduli by microstructure homogenisation, was presented by Biancolini and Brutti (2003). Equivalent moduli evaluation for corrugated board was then formalised by Biancolini with a rigorous numerical procedure based on reduced FEM stiffness matrix (Biancolini 2005). The same procedure was applied by this author for the estimation of corrugated board actual moduli based on image processing (Biancolini 2005).

In this paper a numerical study of buckling and post buckling behaviour of rectangular corrugated board panels simply supported and subjected to compression load is presented. In order to quantify the effect of design parameters on the strength of a panel of given geometry two FEM models at increasing detail level were used: in the first corrugated board was modelled by means of equivalent shell elements, in the second each paper layer is modelled by means of shell elements considering actual properties and shape.

A preliminary study of convergence with mesh size was performed for full detailed model to achieve the best computational efficiency. Optimal mesh was then used for the subsequent calculations.

The models correctness was checked by the comparison between out of plane central displacement predicted by the models and the experimental and theoretical values found in literature (Nordstand 2004). For the same case a sensitivity analysis was performed changing the panel planarity error in the range observed experimentally (i.e. -0.8 mm $\pm$ 0.4 mm). The effect of design parameters was then investigated varying panel composition and shape adopting the same dataset used in (Biancolini 2005).

2. Theoretical background

Investigated panels are built with single wall corrugated board composed by three layers: two external facings and an internal fluting as depicted in Fig. 1, where material directions are also denoted. It is important to notice that material nomenclature is the same of the building papers that have the best performances in the machine direction (MD) since there is a trade off between the achievement of good cross direction (CD) and speed (and cost) of manufacturing. Such anisotropy has to be taken into account in structural modelling. The transversal section with microgeometric parameters is represented in Fig. 2.

As demonstrated in (Mckee *et al.* 1963) the buckling strength of the panel is related to flexural stiffness according to Eq. (3).

$$P_{buck} = 12 \cdot k_{cr} \frac{\sqrt{D_{11} D_{22}}}{W^2} \tag{3}$$

Extending this collapse model to the lateral walls of a container Eq. (3) can be used to estimate the ultimate compression load of a box via the empirical relation expressed in Eq. (4) that considering typical values of the constants reduces to the design formula of Eq. (1).

$$P_{crit} = c \cdot ECT^b P_{buck}^{1-b} \tag{4}$$

As demonstrated by Nordstrand (2004), in the full range of panel compression, considering pre and post

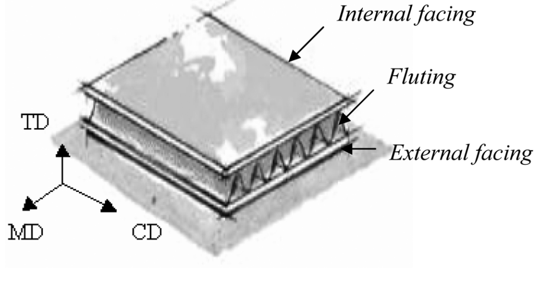

Fig. 1 Corrugated board geometry and material directions

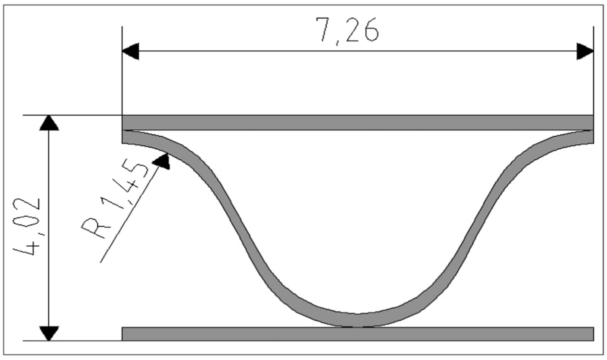

Fig. 2 Corrugated board local geometry in mm

buckling, the following formula for the out of plane displacement at the centre of the panel holds:

$$P = P_{buck}\left(1 - \frac{A_0}{A}\right) + \Psi(A^2 - A_0^2) \tag{5}$$

As exposed in the introduction, corrugated board panels were analysed at two detail levels: considering the corrugated board material as an equivalent shell or modelling the three layers with the actual geometry.

For the estimation of equivalent shell stiffness several approaches can be considered. They can be measured experimentally. They can be calculated by means of the lamination theory, modelling each of the external facing as a uniform orthotropic lamina but special care is required to represent the corrugated core as an equivalent material. They can be directly calculated by means of an homogenisation algorithm based on FEM modelling of local microgeometry.

Local microgeometry modelling is also required for the full detailed FEM model. In this case each layer is modelled by means of orthotropic shell elements taking into particular care the proper material orientation. Such approach allows to predict failure directly from paper materials strength constants, according to Tsai Wu failure criteria recalled in Eq. (2), where the failure occurs when the Failure Index (FI) is greater than one.

$$\begin{aligned} FI &= \Gamma_1\sigma_x + \Gamma_2\sigma_y + \Gamma_{11}\sigma_x^2 + \Gamma_{22}\sigma_y^2 + \Gamma_{66}\tau_{xy}^2 + 2\Gamma_{12}\sigma_x\sigma_x \le 1 \\ \Gamma_{11} &= -\frac{1}{\sigma_{x,t}\sigma_{x,c}};\Gamma_{22} = -\frac{1}{\sigma_{y,t}\sigma_{y,c}};\Gamma_{12} = -0,36\sqrt{E_{11}E_{22}} \\ \Gamma_1 &= \frac{1}{\sigma_{x,t}} + \frac{1}{\sigma_{x,c}};\Gamma_2 = \frac{1}{\sigma_{y,t}} + \frac{1}{\sigma_{y,c}};\Gamma_{66} = \frac{1}{\sigma_{x,c}\sigma_{y,c}}. \end{aligned} \tag{6}$$

The interaction value of 0.36 is recommended in reference (Nordstrand 2004) for paper material.

It’s important to notice that for full detailed model both microgeometry instability and global buckling are simultaneously covered and physically simulated. The proper evaluation of failure for the equivalent shell is a delicate task and it will not further pursued in this work.

2.1. Reference case description

As mentioned in the introduction, this work is focused on the compression strength of a simply supported panel of a given geometry. A useful reference case was found in a literature contribution by Nordstrand (2004) where a complete description of experiments was given. In this reference case a 400 mm side square panel built with single wall corrugated board was investigated.

The special testing device depicted in Fig. 3 was used in order to match the desired simply support constraint at the four edges. Horizontal sides were pinned by means of 25 mm width equal spaced revolution joints along the panel free edge, piecewise clamped to the fixed part of the testing machine at the bottom edge and to the moving crosspiece at the top edge. Lateral sides were pinned by means of knives.

Vertical load and out of plane displacement of the central point were recorded for several panels belonging to the same production lot. The mechanical properties of building papers for reference case are summarised in Table 1. The overall parameters of assembled corrugated board in terms of geometry and tested stiffness are summarised in Table 2.

The load vs out of plane central displacement curves were reported for data resulting from experiments and from a theoretical model based on nonlinear plate theory. The Eq. (5) resulting from the non linear theoretical model was used for the regression of experimental data obtaining the parameters summarised in Table 3.

3. Numerical models description

Two numerical models were developed adopting the finite element solver Nastran. In the first model the corrugated board is represented by means of shell elements. The structure was modelled by means of an equivalent material in order to get the desired flexural matrix D adopting the overall corrugated board thickness h. In the second the local structure is represented in full details modelling both straight and corrugated layers by means of shell elements and representing the connection between layers by rigid elements.

In both cases standard CQUAD4 shell elements are used. A non linear elastic solution is performed activating large displacement options. With this setting 4 nodes iso-parametric large displacements elements are used with a co-rotational algorithm able to substract non-linear rigid body displacements, strains and

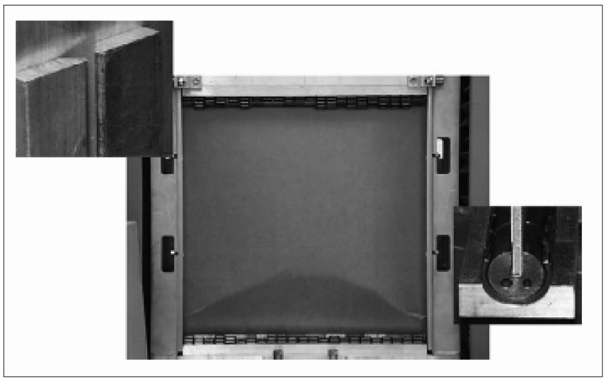

Fig. 3 Reference case test equipment (Nordstrand 2004)

Table 1 Reference case: building papers properties (Nordstrand 2004)

	Direction	Internal facing	Fluting	External facing	Dimension
Density		184.3	140.2	187.4	g/m^2
Thickness		0.268	0.217	0.244	mm
E_{11}	MD	7980	4750	8090	N/mm^2
E_{22}	CD	3190	1560	2490	N/mm^2
$\sigma_{x,t}$	MD	81.4	46.9	82.1	N/mm^2
$\sigma_{y,t}$	CD	28.4	18.8	31.5	N/mm^2
$\sigma_{x,c}$	MD	30.8	23.1	29.9	N/mm^2
$\sigma_{y,c}$	CD	16.6	13.4	16.2	N/mm^2

Table 2 Reference case: corrugated board properties (Nordstrand 2004)

Density	556	g/m^2
Thickness h	3.84	mm
Wave length λ	7.26	mm
Flexural stiffness D_{11}	14.6	N·m
Flexural stiffness D_{22}	5.43	N·m
Flexural stiffness D_{12}	2.71	N·m
Flexural stiffness D_{66}	3.34	N·m

Table 3 Reference case: experimental data regression results (Beldie *et al.* 2001)

	$P_{buck,exp.}$ (N)	A_0 (mm)	Ψ_{exp} (N/mm^2)	$P_{crit,exp.}$ (N)
Mean value	814	0.8	3.55	1195
Standard deviation	16	0.3	0.59	60

stresses are then calculated adopting the standard linear definition of the elements based on the small strains assumption. An incremental load introduction mechanism is adopted selecting the maximum load proportional to buckling load.

Numerical models represent only a quarter of the whole panel. Symmetry simplification is herein applicable because aspect ratio of the investigated panel leads to a symmetric first mode for buckling. Furthermore a comparison between a full model and a quarter model was performed obtaining the same results both for first buckling eigenvalue and for non linear analysis. In Fig. 4 is represented the full detailed FEM model deformed by compression loads. Every paper layer is modelled with shell elements using characteristic moduli and strength coefficients. Due to the symmetry used, two edges of the quarter model are constrained as in the actual panel: all translations out of the plane of the panel are constrained, the other two edges of the model, which in the real panel are 'internal' to the panel itself, are constrained to maintain symmetrical displacements. Special care was taken to properly reproduce the piecewise support using rigid elements to represent the joints as exposed in Fig. 5. The compression load is applied to an external node that model the crosspiece of the testing machine, which is linked to all nodes of the edge with rigid elements in order to transfer the load to the edge.

To properly represent the microgeometry in the detailed model, the length of one wave has been divided in eight segments. This caused, also if only a quarter of the model was modelled, a large number of nodes and elements, which means a large use of calculation resources.

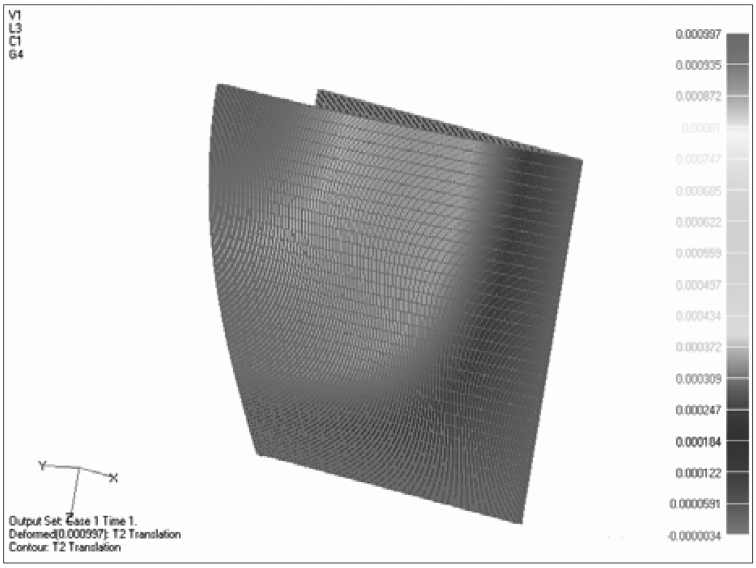

Fig. 4 Corrugated board panel: FEM model deformed shape

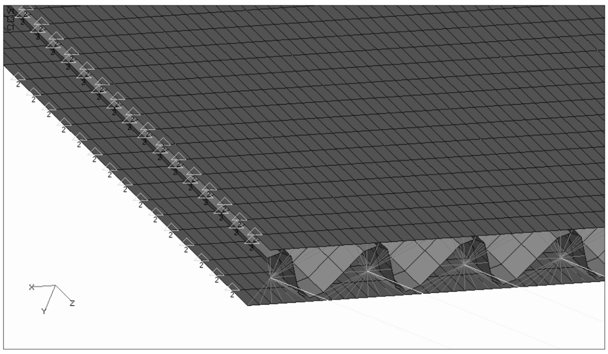

Fig. 5 Corrugated board panel FEM model constraint

3.1. Investigated parameters

In order to illustrate the utility of the proposed numerical model in corrugated board panel design, a parametric analysis was performed. Neglecting the effect of panel geometry, i.e. leaving unaffected the panel dimension, a number of variations in composition and thickness were investigated.

The data set chosen (Biancolini 2005) is summarised in Table 4. The stiffness constants presented in the reference were determined numerically by means of an homogenisation procedure. Their values are collected in Table 4. Building papers properties used for the data set are summarised in Table 5.

Base composition is KLSKL 595 3.8 mm thick that is widely used for the design of BCT constraint boxes. The effect of a worst and less expensive material for fluting (KLSKL 565) for both fluting and facings (TST 565) and for facings (TST 595) was then considered. Last composition variation (KLSKL 696) is an improvement of both materials. With respect to the base composition also the effect of thickness reduction and increment was considered. This is a way to estimate the effect on corrugated board performances of the damage inflicted during case-making and printing. As far as the modelling point of view is concerned thickness variations were imposed by means of scale transformation of transversal nodes positions.

4. Results and discussion

4.1. Mesh optimisation

For full detailed FEM model adopted in this study, the number of degree of freedom is a critical parameter that has to be optimised in order to minimise the computational effort within a prescribed convergence error. For this reason a preliminary convergence analysis was performed to optimise the mesh. Leaving the same number of elements to represent the shape of the wave, five models were realised changing the number of elements and nodes in the cross direction. Table 6 summarises numerical model features. The convergence analysis was performed for the buckling load: to every model was applied the same load and the difference between results was evaluated, in order to check which model gives most accurate results using less resource as possible. Subsequent analyses were performed with model C that allows a CPU speedup factor equal to 41 with a convergence error of 3%.

4.2. Model validation

Once the FEM model mesh density was optimised a set of calculations were performed to validate the numerical model against the reference case. The first check performed was the evaluation of flexural stiffness by means of the full detailed FEM model of microgeometry. Adopting a square portion of the

Table 4 Parametric analysis: corrugated board properties

Case #	1	2	3	4	5	6	7	Units
Thickness	3.8	3.8	3.8	3.8	3.8	3.5	4.1	mm
Composition	KLSKL 595	KLSKL 565	TST 565	TST 595	KLSKL 696	KLSKL 595	KLSKL 595	
D_{11}	6.438	6.069	4.593	4.874	7.266	5.393	7.577	N·m
D_{22}	4.143	3.793	3.03	3.335	4.985	3.449	4.905	N·m
D_{12}	1.103	1.099	1.037	0.793	0.845	1.324	0.924	N·m
D_{33}	1.779	1.648	1.28	1.388	2.074	1.49	2.093	N·m

Table 5 Parametric analysis: building papers properties

	t	ρ	E_{11}	E_{22}	G_{12}	ν_{12}	σ_{tMD}	σ_{tCD}	σ_{cMD}	σ_{cCD}	τ	RCT
Name	mm	g/m^2	MPa	MPa	MPa		MPa	MPa	MPa	MPa	MPa	kN/m
KL 3	0.20	150.0	3940.6	1656.1	784.3	0.34	49.53	18.12	11.25	6.50	8.55	1.30
KL 5	0.29	200.0	3326.4	1694.5	728.8	0.34	41.27	19.47	14.08	8.14	10.70	2.36
KL 6	0.32	230.0	3292.7	1694.5	725.2	0.34	41.39	20.70	13.57	7.84	10.32	2.51
T 5	0.29	185.0	2499.8	1256.1	544.0	0.34	24.63	12.81	10.20	5.90	7.76	1.71
S 6	0.25	150.0	3226.2	1610.0	699.7	0.34	33.35	14.48	9.83	5.68	7.47	1.42
S 9	0.30	175.0	2614.8	1532.2	614.5	0.34	32.71	14.94	11.07	6.40	8.42	1.92

Table 6 FEM models used in convergence analysis

Model	Nodes #	Elements #	CPU (sec)	Speedup	P_{buck} (N)	P_{crit} (N)	Error (%)
A	89273	95657	18826.0	1	886.4	1772.9	0
B	44651	47484	2196.8	9	876.2	1752.4	1
C	22007	23038	454.2	41	857.6	1715.2	3
D	11351	11534	169.3	111	816.7	1633.3	9
E	6023	5782	87.0	216	727.5	1455.0	22

model and the homogenisation algorithm reported in (Biancolini 2005) the values of Table 7 were obtained. Numerical values match very well the reference values of Table 2.

A comparison with experimental data was then conducted adopting the nominal initial imperfection of −0.8 mm in the detailed FEM model. Central point out of plane displacement against load was selected as the non linear synthetic parameter of panel collapse. Experimental reference curve was computed inserting mean values of data regression summarised in Table 3 in Eq. (5). In Fig. 6 experimental curve and theoretical curve presented in the reference are represented and compared with the numerical results obtained with both FEM models.

As can be noticed the theoretical curve show a close agreement with the one calculated by the simple FEM model. This is a first confirmation of modelling correctness because both results are based on the same theory. It is worthwhile to notice that both theoretical and simplified FEM models neglects the contribution of the coupling introduced by the asymmetric lamination of the sandwich structure.

A very good agreement is observed between the experimental curve and the one calculated by the detailed FEM model. The detailed model seems capable to reproduce the actual deformation for the panel in the postbuckling regime. As far as the failure assessment of the panel is concerned, having modelled the three materials with a linear orthotropic constitutive law, a correct failure criterion has to be selected. The best choice seems to use the maximum failure index calculated according to Eq. (6) as a damage measure and to use the value at the load of experimental as limit condition. Calculating the failure index with respect to ultimate stress of Table 1 a 0.3 failure index at panel collapse results. The failure index map is represented in Fig. 7 at buckling load level and at collapse load level. It is interesting to observe the ability of the panel to resist after the buckling load transferring the carrying capacity mainly to the regions near the corners. Furthermore the maximum damage map calculated by the model agree very well with the actual damage observed in the panel at collapse depicted in the same Fig. 7.

4.3. Effect of panel initial deflection

Initial deflection due to panel planarity error was first set to be equal to −0.8 mm in the model validation analysis. In order to quantify the effect of this parameter on pre e post buckling stages a sensitivity

Table 7 Validation of method: flexural stiffness

	Reference	Calculated	
Flexural stiffness D_{11}	14.6	14.63	N·m
Flexural stiffness D_{22}	5.43	5.905	N·m
Flexural stiffness D_{12}	2.71	2.553	N·m
Flexural stiffness D_{66}	3.34	3.270	N·m

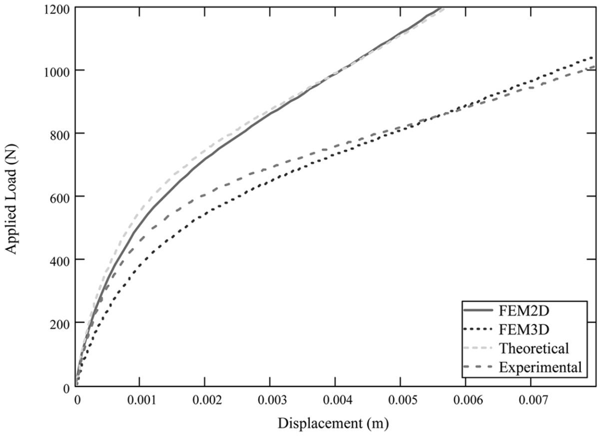

Fig. 6 Displacement of central point of panel versus applied load: experimental results, theoretical model, simple FEM model (FEM2D), detailed FEM model(FEM3D)

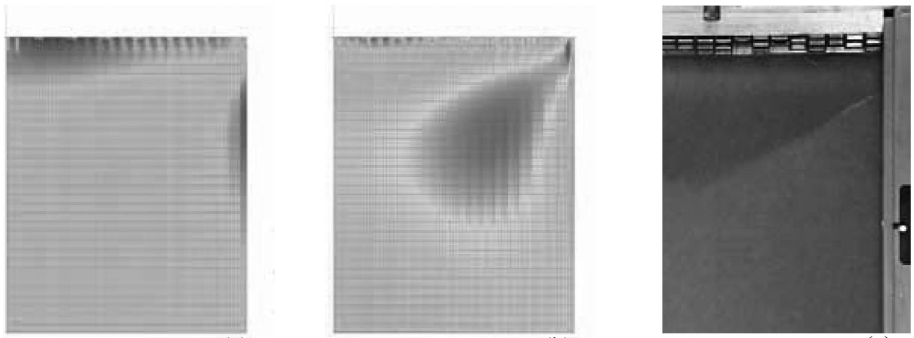

Fig. 7 Damage evolution. At buckling the maximum failure index is located at the corner (a), in the post buckling regime damage extends to the large deformation region (b) exhibiting a distribution almost identical to the experimental (c)

analysis was conducted varying the value of this parameter in its experimental range reported in Table 3. Furthermore to account for sandwich asymmetry, both positive and negative values were considered. A positive value means that the initial displacement is in the direction of the Internal facing. Investigated values are summarised in Table 8. As can be observed by the Table the first eigenvalue is affected by the initial imperfection and also the lateral displacement curves reported in Fig. 8 show a quite different behaviour, especially changing the direction of the initial imperfection. Furthermore a better match between numerical and experimental values is observed if the initial imperfection is considered positive and equal to 0.4 mm. The last observation is also confirmed by the integrated quadratic difference between numerical and experimental curves that is minimum for the aforementioned value (Table 8).

4.4. Parametric analysis results

In the remainder of this discussion the results of the parametric analysis are presented. It is important

Table 8 Initial planarity error analysis, quadratic error is computed with respect to the experimental curve

Case #	1	2	3	4	5	6	7	Units
A_0	−1.2	−0.8	−0.4	0	0.4	0.8	1.2	mm
P_{buck}	874.3	857.6	846.6	841.4	841.7	847.7	859.4	N
Quadratic error	40.9	13.8	1.4	32.1	219.7	213.6	66.2	n.a.

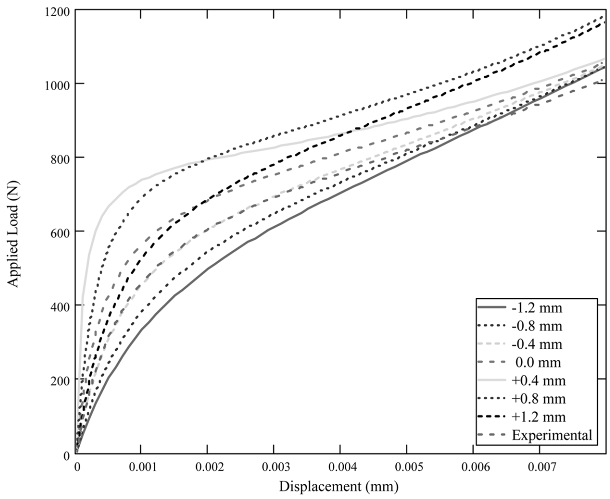

Fig. 8 Displacement of central point of panel versus applied load: effect of initial planarity error computed by means of detailed FEM model and comparison with experimental curve

to notice that all the analyses were performed considering the corrugated boards summarised in Table 4 using the full detailed FEM model of the panel and the max failure index value of 0.3 to identify failure according to the comparison between experimental and numerical results for the reference case. Furthermore the initial deflection due to panel planarity error was left constant and equal to its nominal value. In Fig. 9 predicted deflection curves obtained for investigated compositions are depicted. As expected stiffness variations due to building materials reflect themselves in stiffness variations of the panel with a strong contribution of the facings materials and a little contribution of the core material. However such interpretation may lead to a wrong prediction because a better core material allows to preserve panel thickness during manufacturing as discussed in (Biancolini 2005). Last consideration is well supported by results of Fig. 10 were the effect of thickness is reported. The same trend is observed in maximum failure index (Figs. 11 and 12) showing better performances for high quality paper and higher thickness. Obtained results were processed to obtain buckling loads (row 4 of Table 9) and critical loads (row 6 of Table 9).

Relative differences with the baseline configuration of the first column are also highlighted (rows 5 and 7 of Table 9). As foresaw by Eq. (3), the combined flexural stiffness parameter (row 2 of Table 9) results as a good estimator for buckling. It exhibits the same trends (its variation with respect to the baseline are reported in row 3 of Table 7) of computed buckling value. Furthermore, with exception of Case 2 (KLSKL 565) for which the combined flexural stiffness parameter overestimates the reduction in buckling load, also the amount of gain or loss is similar.

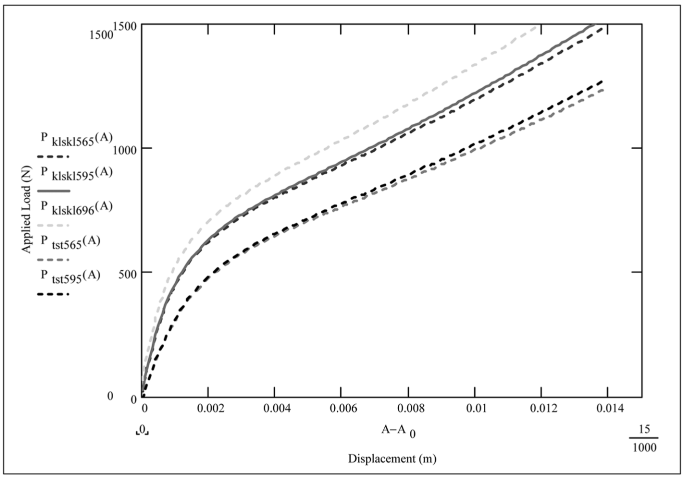

Fig. 9 Parametric analysis, displacement of central point of panel versus applied load changing composition

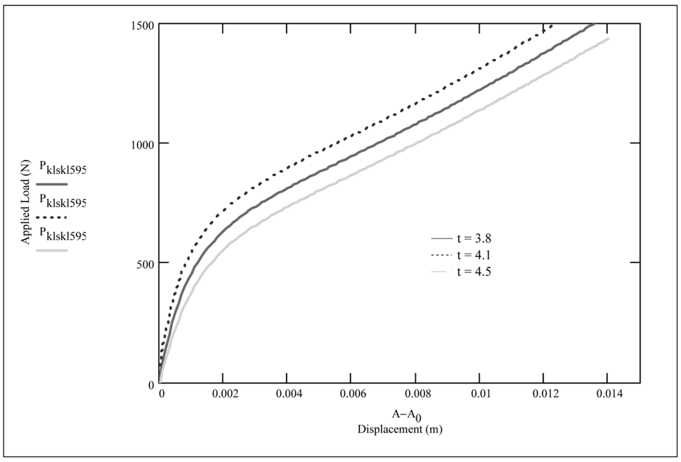

Fig. 10 Parametric analysis, displacement of central point of panel versus applied load changing thickness

As far as the failure load is concerned it's very important to notice that different compositions produce changing both in panel stiffness and in strength because of different thickness, stiffness moduli and ultimate stress values. For this reason, although the same trends could be expected, the amount of changing may be quite different as shown in the Table. In fact for Case 5 (KLSKL 696) despite the higher stiffness an improvement lower than 1% is predicted in panel strength and for the case 7 (thickness increment) the gain in collapse strength predicted by buckling load results halved in terms of panel strength.

5. Conclusions

In this paper a numerical model for corrugated board panel strength prediction was presented. The

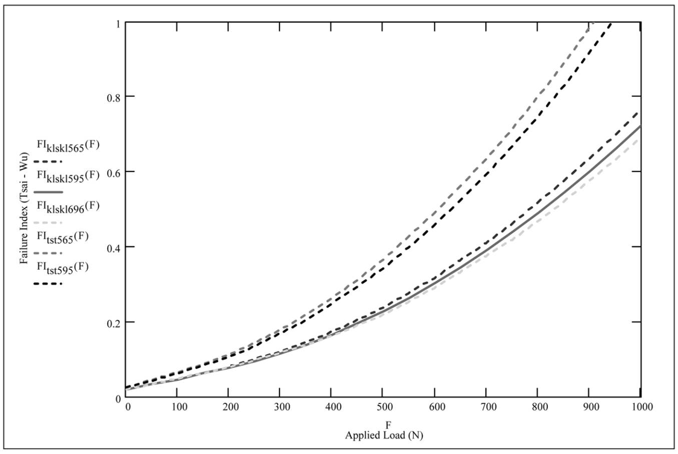

Fig. 11 Parametric analysis, damage index versus applied load changing composition

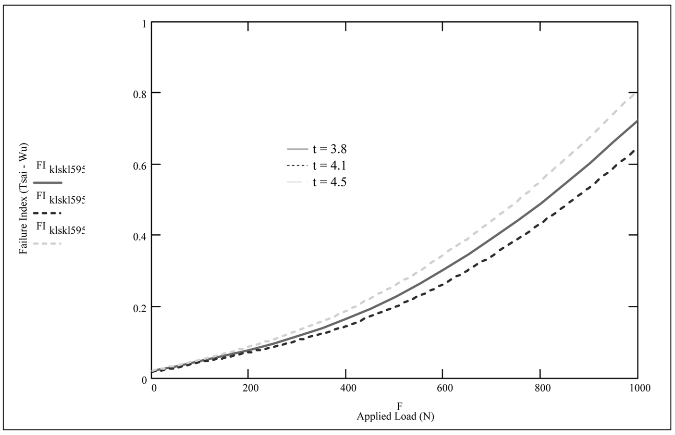

Fig. 12 Parametric analysis, damage index versus applied load changing thickness

Table 9 Parametric analysis results

Case #	1	2	3	4	5	6	7	Units
$\sqrt{D_{11} \cdot D_{22}}$	5.156	4.798	3.731	4.032	6.018	4.313	6.096	N·m
$\Delta\sqrt{D_{11} \cdot D_{22}}$	0.00	−7.10	−27.77	−21.93	+16.53	−16.49	+18.04	%
P_{buck}	1000.5	988.2	718.2	727.5	1136.9	849.8	1163.0	N
Δ P_{buck}	0	−1.2	−28.2	−27.4	+13.6	−15.2	+16.2	%
P_{crit}	1211.8	1173.3	890.1	927.1	1221.4	1117.2	1312.4	N
Δ P_{crit}	0	−3.2	−26.6	−23.5	+0.8	−7.8	+8.25	%

model was validated with respect to a literature reference solution based both on experimental and theoretical results. Full detailed FEM model produces out of plane displacement curve in the full non linear range, covering the transition between buckling and post buckling regions, near to the experimental results.

The model was used to investigate the effect of initial imperfection and for a parametric analysis changing the composition and the overall thickness. A good agreement was found between calculated buckling loads and the values estimated on the basis of combined flexural stiffness parameter. The same trend was found in the collapse load, but with different amount in variations because the result is a combination of both stiffness and strength variations.

Proposed tool seems quite interesting for corrugated board panel design optimisation and can be used both for the definition of an optimal set of composition and as an everyday calculation tool for corrugated material design.

Acknowledgements

The authors would like to express their acknowledgements to Riccardo Di Veroli and Giovanni Toti of Smurfit Group for the practical support of this research and for their invaluable suggestions.

References

Aboura, Z., Talbi, N. Allaoui, S. and Benzeggagh, M. L.(2004), "Elastic behaviour of corrugated cardboard: experiments and modeling", *Compos. Struct.,* **63**, 53-62.

Beldie, L., Sandberg, G. and Sandberg, L. (2001), "Paperboard packages exposed to static loads-finite element modelling and experiments", *Packag. Technol. Sci*, **14**(4), 171-178.

Biancolini, M. E. (2005), "Evaluation of equivalent stiffness properties of corrugated board", *Compos. Struct.*, **69**(3), 322-328.

Biancolini, M. E. (2005), "On line quality control of corrugated board panel by image processing", *Int. J. Computer Applications in Technology*, **23**(2/3/4), 157-165.

Biancolini, M. E. and Brutti, C. (2003), "Numerical and experimental investigation of the strength of corrugated board packages", *Packag. Technol. Sci.*, **16**(2), 47-60.

Gilchrist, A. C., Suhling, J. C. and Urbanik, T. J. (1999), *Nonlinear finite element modeling of corrugated board*, American Society of Mechanical Engineers - Applied Mechanics Division (AMD), **231**, 101-106.

Lu, T. J., Chen, C. and Zhu, G. (2001), "Compressive behaviour of corrugated board panels", *J. Compos. Mater.*, **35**(23), 2098-2126.

McKee, C., Gander, J. W. and Wachuta, J. R. (1963), *Compression Strength Formula for Corrugated Boxes.*, Paperboard Packaging, 149-159.

Nordstrand, T. (2004), "Analysis and testing of corrugated board panels into the post-buckling regime", *Compos. Struct.,* **63**, 189-199.

Nordstrand, T. and Carlsson, L. A. (1997), "Evaluation of transverse shear stiffness of structural core sandwich plates", *Compos. Struct.*, **37**, 145-153.

Pommier, J. C. and Poustis, J. S. (1990), *Bending stiffness of corrugated board prediction using the finite elements method*, American Society of Mechanical Engineers - Applied Mechanics Division (AMD), **112**, 67-70.

Appendix 1: Notation.

Symbol	Description	Dimensions
A_0	Initial panel out of plane central deflection	mm
A	Panel out of plane central deflection	mm
P_{buck}	Buckling load	N
P_{crit}	Critical load at panel collapse	N
Ψ	Post buckling parameter	N/mm^2
k_{cr}	Buckling parameter	1.33
W	Panel width	mm
ECT	Strength of a rectangular corrugated board specimen in Edge Compression Test	kN/m
$c,\ b$	McKee formula empirical constants	0.5, 0.746
σ_x	Stress in MD	MPa
σ_y	Stress in CD	MPa
τ_{xy}	Shear stress in reference MD, CD	MPa
$\sigma_{x,c}$	Ultimate compression stress in MD	MPa
$\sigma_{y,c}$	Ultimate compression stress in CD	MPa
$\sigma_{x,t}$	Ultimate tensile stress in MD	MPa
$\sigma_{y,t}$	Ultimate tensile stress in CD	MPa
τ	Ultimate shear stress in reference MD, CD	MPa
RCT	Strength of a ring strip of paper specimen in Ring Compression Test	kN/m
ρ	Surface density	kg/m^2
t	Paper thickness	mm
E_{11}	Young modulus in MD	MPa
E_{22}	Young modulus in CD	MPa
G_{12}	Shear modulus in reference MD, CD	MPa
ν_{12}	Poisson modulus in reference MD, CD	m/m
D_{11}	Flexural stiffness in MD	N·m
D_{22}	Flexural stiffness in CD	N·m
D_{12}	Flexural stiffness coupling in reference MD, CD	N·m
D_{33}	Torsional stiffness in reference MD, CD	N·m
h	Corrugated board global thickness	mm
BCT	ultimate compression load obtained in Box Compression Testing	kg
p	box perimeter	cm
ψ	wave corrugation ratio	

Appendix 2: Paper and corrugated board designation.

Corrugated board is usually designed with type and density of building papers and with fluting shape, according to the syntax:

Lci Lf Lce Di De Df Ls (for instance KSK595C)
Where

Lci and **Lce** are letter denoting the kind of paper used for internal and external facing (Table I)
Di and **De** are number denoting the density of paper used for internal and external facing(Table II)
Lf is a letter denoting the kind of paper used for fluting (Table III)
Df is a number denoting the density of paper used for fluting (Table IV)
Ls is a letter denoting the kind of wave used for fluting (Table V)

Table I Facing paper designation

Symbol	Paper
K	Kraft
L	Liner
T	Test-liner
Kb	Kraft bianco
Lb	Liner bianco
Tb	Test bianco

Table II Facing paper density grades

Grade	2	3	4	5	6	8	9	02	04	06
Density (g/m^2)	125	150	175	200	225	275	300	337	400	440

Table III Fluting paper designation

Symbol	Paper
S	Semichimica
M	Medium
F	Fluting

Table IV Fluting paper density grades

Grade	2	4	6	9
Density S,M (g/m^2)	112	127	150	180
Density F (g/m^2)	120	145	170	210

Table V Wave profile code and corrensponding geometric parameter

Wave profile	Corrugated board thickness (mm)	Wave pitch (mm)	Number of wave for meter	Corrugation factor
Wide (A)	> 4.5	8.6 ÷ 9.1	110 ÷ 116	1.48 ÷ 1.52
Short (B)	2.5 ÷ 3.4	6.3 ÷ 6.6	152 ÷ 159	1.33 ÷ 1.36
Medium (C)	3.5 ÷ 4.4	7.3 ÷ 8.1	123 ÷ 137	1.41 ÷ 1.45
Micro (E)	< 2.5	3.2 ÷ 3.4	294 ÷ 313	1.23 ÷ 1.30

Several type of corrugated board panel are produced in the same plant, they differ in number of layers, building material of each layer and fluting shape of each corrugated layer. Packaging designer has to choose the best composition for each product looking for the lower cost solution that meets design requirements. The wave shape is chosen according to the following guidelines:

Wave A is used to produce high thickness corrugated board (>4.5 mm) that is difficult to print because a waviness remain in the external facing for the high pitch values adopted; the worst ECT values are usually exhibited by this shape. High bending stiffness is obtained.

Wave B has little thickness (2.5-3.4), little ECT value and low bending stiffness value. The little thickness produces high lateral crushing strength and the low pitch values involved bring a good planarity that makes easy to print the corrugated board

Wave C is the geometry usually adopted for the building of container subjected to compression loads, the medium thickness is the best trade-off between mechanical performance and paper consumption.

Wave E usually is used in combination with other shapes to build triple wall corrugated board (E+B). A smooth external surface is obtained with high aesthetic quality and easy to print.

CC